Frontiers in Scientific Research and Technology

Online ISSN: 2682-2970
Print ISSN: 2682-2962
http://fsrt.journals.ekb.eg

FSRT J 5 (2023) 111-123 10.21608/FSRT.2023.190393.1082

On HIV Mathematical Model; Numerical Approaches

N. H. Sweilam [1]*, Z. N. Mohammed [2], W. S. Abdel Kareem [2]

[1] Department of Mathematics, Faculty of Science, Cairo University, Giza, Egypt

[2] Department of Mathematics, Faculty of Science, Suez University, Suez, Egypt

ARTICLE INFO

Article history:
Received 11 February 2023
Accepted 14 March 2023
Available online 22 March 2023

Keywords
Complex order HIV infection model,
Nonstandard two-step Lagrange interpolation method,
Standard two-step Lagrange interpolation method,
Atangana-Baleanu complex order derivative,
Drug resistance.

ABSTRACT

In this article, numerical approaches for a complex order mathematical model for HIV that includes drug resistance across the course of therapy are presented. HIV is a virus that weakens the immune system, making a person more susceptible to infections and diseases. This model consists of five nonlinear complex order differential equations where the derivatives is specified in the sense of Atangana-Baleanu-Caputo. Mittag-Leffler kernels are used in new numerical approaches to simulate complex order systems. These methods are based on Lagrange polynomial interpolation and the fundamental theorem of fractional calculus. For the two-step Lagrange polynomial interpolation, we suggest a straightforward adjustment to the step size to achieve high stability. The stability of the disease free equilibrium point of the proposed model is presented. The complex order HIV model is mathematically studied using two different techniques: the standard and nonstandard Two-step Lagrange interpolation methods, which are suggested. To support the theoretical foundations, comparative investigations and numerical simulations are provided.

1. Introduction

HIV is a virus that damages the body's immune system, increasing a person's susceptibility to illnesses and infections. It is transmitted through coming into touch with the bodily fluids of HIV-positive individuals, most frequently during unprotected sexual contact, or by exchanging injectable drug apparatus. HIV cannot be eliminated by the body and there is no effective treatment for it.

Nowadays, mathematical models are widely acknowledged as a trustworthy method for verifying experiments, evaluating hypotheses, and simulating complicated system dynamics.

The history or memory of the variable can be recorded using fractional derivatives, which is a special quality. Additionally, current memory has a stronger impact than earlier history [33]. Using derivatives of integer order is challenging. Since integer order derivative models are less accurate when compared to fractional derivative models when using real data, their usage is warranted for resolving a range of issues.

In contrast to fractional and complex order derivatives, integer-order derivatives are unable to account for systems that are affected by inherent qualities of materials and techniques as well as history memories ([3],[38]). Recently, Atangana-Baleanu Caputo (ABC) defined an improved Caputo fractional derivative by substituting a generalised Mittag-Leffler function for the nonlocal kernel and non-singular [14]. These current versions have been utilised in a variety of disciplines to represent real-world applications.

The fractional order derivative and the integer order derivative are recognised as having gained popularity as a result of the complex order derivative when the imaginary part of the complex order equals zero [11]. A unique mathematical model focused on a complex order model was presented by Pinto and Carvalho in [3] for HIV infection with treatment resistance. They came to the realization that the complex order system has a number of benefits, including rich dynamics and the ability to add new information to the modelling work of intracellular delay by changing the complex order derivative value. Additionally, Pinto and Machado suggest the forced van der Pol oscillator in [22] as a complex-order approximation. Also, Sweilam et al. in [39] devised a technique for dealing with the complex order mathematical formula of HIV with treatment resistance over the course of treatment.

This work's main contribution is the development of a productive numerical technique for approximating the

* Corresponding author at Cairo University
E-mail addresses: nsweilam@sci.cu.edu.eg (N. H. Sweilam)

solutions of the complex order HIV model, which is presented in [3]. When compared to the standard two-step Lagrange interpolation method (S2LIM), the nonstandard two-step Lagrange interpolation method (NS2LIM) performs better [1]. On offer are numerical simulations for the complex order model.

The article is divided into the following sections: In Section 2, the complex order calculus are introduced. The HIV model is described in section3 in a complex order. In section 4, the stability of the disease free equilibrium point of the proposed model is presented. In section 5 NS2LIM is discussed. The numerical method for the presented utilising NS2LIM is described in section 6. In section 7, numerical simulations are utilised to show the effectiveness and applicability of the NS2LIM. Finally, section 8 contains the conclusions.

2 Preliminaries and Notations

The basic definitions of complex order calculus that will be used in this artical are covered in this section.

2.1 Complex Order Calculus

The following is the general form of the complex order ordinary differential equation:

$$ {}_{0}^{ABC}D_{s}^{z}x(s) = g(s, x(s)), \quad x(0) = x_0, \quad z \in \mathbb{C}. \tag{1} $$

Definition 2.1 *For complex order derivatives of a function $g(t)$, the Caputo formula is as follows $z \in \mathbb{C}$ [18]:*

$$ {}_{0}^{C}D_{s}^{z}g(s) = \begin{cases} {}_{0}^{C}D_{s}^{z-\lceil Re(z)\rceil}\,{}_{0}^{C}D_{s}^{\lceil Re(z)\rceil}g(s),\ z \notin \mathbb{N}\ \ and\ \ Re(z) \in \mathbb{R}^{+}, \\ \dfrac{d^{z}g(s)}{ds^{z}},\ \ if\ \ z \in \mathbb{N}, \\ {}_{0}^{C}D_{s}^{z-1}g(s),\ \ if\ \ \Im(z) \neq 0\ \ and\ \ Re(z) = 0, \\ \dfrac{1}{\Gamma(1-z)}\displaystyle\int_{0}^{s}\frac{g'(s)}{(s-r)}dr,\ \ if\ \ Re(z), Im(z) \in \mathbb{R}, \\ g(s),\ \ if\ \ z = 0, \\ \displaystyle\int_{0}^{s}\frac{(s-r)^{-z-1}}{\Gamma(-z)}g(r)dr,\ \ if\ \ Re(z) \in \mathbb{R}^{-}. \end{cases} \tag{2} $$

The gamma function appears as follows for $z \in \mathbb{C}$ [7]:

$$ \Gamma(z) = (2\pi)^{\frac{1}{2}}e^{-z}z^{z-\frac{1}{2}}[O(\frac{1}{z})+1],\ |z| \to \infty, |arg(z)| < \pi. \tag{3} $$

Definition 2.2 *For complex order derivatives of a function $g(t)$, the Grünwald-Letinkov formula (GL) is as follows $z \in \mathbb{C}$:*

$$ {}_{a}^{GL}D_{s}^{z}g(s) = \lim_{h\to 0}\frac{1}{h^{z}}\sum_{j=0}^{[\frac{s-a}{h}]}(-1)^{j}\binom{z}{j}g(s-jh), \tag{4} $$

the integer portion of $\dfrac{s-a}{h}$ is denoted by $[\dfrac{s-a}{h}]$, the bounds of operation for ${}_{a}D_{s}^{z}g(s)$ are a and s, see [18] for more information.

Definition 2.3 *For complex order derivatives of a function $g(t)$, the Atangana-Baleanu complex order derivative (ABC) in the Liouville-Caputo senses is defined as follows [5]:*

$$ {}_{0}^{ABC}D_{s}^{z}g(s)=\frac{B(z)}{2\pi i(1-z)}\int_{0}^{t}E_{z}[-z\frac{(s-r)^{z}}{1-z}]g^{'}(r)dr,\ \ z\in\mathbb{C}, \tag{5} $$

where $Re(z)>0$ and $B(z)=\frac{z}{\Gamma(z)}-z+1$, and E_z is the Mittag-Leffler function:

$$ E_{z}(Y)=\sum_{m=0}^{\infty}\frac{Y^{n}}{\Gamma(zm+1)},\quad Y,\ z\in\mathbb{C}. $$

3. The Mathematical Model

In the following the complex fractional order HIV model is considered. This model proposed by Pinto and Carvalho in [3] and sweilam et al studied HIV in a complex order in [39]. This model consists of five nonlinear complex fractional order differential equations. The definitions of each variable in the suggested model are listed in table 1. Table2 also introduces the parameters and their interpretation for the suggested model. The target cells T that are not infected are listed as follows [4] :

$$ G(s)=\begin{cases} G_{1}(s)=(\lambda-dT)+r(1-\frac{T}{T_{max}}),\\ G_{2}(s)=r(1-\frac{T_{r}+T+T_{s}}{T_{max}})+(\lambda-dT),\\ G_{3}(s)=(\lambda-dT). \end{cases} \tag{6} $$

Table 1: Variables in the model [3].

Variable	Definition
T	Uninfected $CD4^{+}T$ populations cells
T_s	drug-sensitive cells with infection
T_r	drug-resistant cells that are infected
V_s	virulent, medication-sensitive pathogens
V_r	viruses that are contagious and resistant to medication

Following is a description of the complex order model:

$$ \frac{1}{2}(D^{e+if}+D^{e-if})T(s)=-((1-n_{rt}^{s})k_{s}T(s)V_{s}(s)-k_{r}(n_{rt}^{r}-1)T(s)V_{r}(s)-G(T)), $$

$$ \frac{1}{2}(D^{e+if}+D^{e-if})T_{s}(s)=-((1-u)k_{s}(n_{rt}^{s}-1)T(s)V_{s}(s)+\delta T_{s}(s)), $$

$$ \frac{1}{2}(D^{e+if}+D^{e-if})V_{s}(s)=-(cV_{s}(s)+N_{s}\delta(n_{p}^{s}-1)T_{s}(s)), $$

$$ \frac{1}{2}(D^{e+if}+D^{e-if})T_{r}(s)=-(\delta T_{r}(s)+uk_{s}(n_{rt}^{s}+1)T(s)V_{S}(s)+k_{r}(\eta_{rt}^{r}-1)T(s)V_{r}(s)), $$

$$ \frac{1}{2}(D^{e+if}+D^{e-if})V_{r}(s)=-(N_{r}\delta(n_{p}^{r}+1)T_{r}(s)+cV_{r}(s)). \tag{7} $$

Table 2: Parameters in the model [3]

Parameter	Value	Definition
λ	75	the frequency of T cell synthesis.
δ	1	Infected cell death.
T_{max}	1500	carrying capacity of T .
r	0.03	The T gene's rate of proliferation.
k_s	2.4×10^{-6}	The percentage of V_s infections.
n_p^s	0.1	Wildtype strain's PI effectiveness.
k_r	2×10^{-6}	The percentage of V_r infections .
n_{rt}^s	0.4	RTI's rate effectiveness for wild type.
u	3×10^{-5}	Proliferation of the T virus (without the virus or infected T cells).
d	0.1	The fatality rate of T .
c	23	viral clearance rates, in percentage terms.
N_s	4800	Drug-sensitive strain bursting sizes.
N_r	4000	Drug-resistant strain bursting sizes.
n_{rt}^r	0.2	RTI's rate effectiveness for mutants.
n_p^r	0.1	PI's effectiveness in treating mutations.

4 Stability of the Disease-Free Equilibrium Point

According to [3], more information on how to compute the disease-free equilibrium point can be found. The absence of all diseases is referred to as the disease-free equilibrium. In the following the free Equilibrium point is locally asymptotically stable [39]. In equation(7) we put

$$\frac{1}{2}({}_0^{ABC}D^{e+if} + {}_0^{ABC}D^{e-if})T(s) = 0,$$

$$\frac{1}{2}({}_0^{ABC}D^{e+if} + {}_0^{ABC}D^{e-if})T_s(s) = 0,$$

$$\frac{1}{2}({}_0^{ABC}D^{e+if} + {}_0^{ABC}D^{e-if})V_s(s) = 0,$$

$$\frac{1}{2}({}_0^{ABC}D^{e+if} + {}_0^{ABC}D^{e-if})T_r(s) = 0,$$

$$\frac{1}{2}({}_0^{ABC}D^{e+if} + {}_0^{ABC}D^{e-if})V_r(s) = 0,$$

and $T_r = 0$ then we solve the obtained algebraic system to have the disease-free equilibrium point ξ_1 of HIV model (7) as follows:

$$\delta_1 = (\frac{r+\lambda}{\frac{r}{T_{max}}+d}, 0, 0, 0, 0).$$

Evaluation of the Jacobian matrix at the free equilibrium point in [39] then the characteristic equation is given as follows:

$$D^5 + 53.1D^4 + 820.2138D^3 + 3101.6195D^2 + 4381.3044D + 2082.0898 = 0. \quad (8)$$

Then the eigenvalues are given by,

$$D_1 = -0.0500, \quad D_2 = -11.5973, \quad D_3 = -0.4027, \quad D_4 = -11.6051,$$

$$D_5 = -0.3949.$$

Therefore, when D_1, D_2, D_3, D_4 and $D_5 \leq 0$, the model's free equilibrium point is asymptotically stable. If all the eigenvalues D_i of the Jacobian matrix $J = \frac{\partial g}{\partial t}$ which calculated at the equilibrium point are satisfy $|arg(D_i)| > \frac{|e \pm if)|\pi}{2}$, and $0 < |e \pm if| \leq 1$ Consequently, the equilibrium point is asymptotically stable locally.

5. Numerical Technique

In numerical analysis, Lagrange polynomials are applied for polynomial interpolation. For a specified collection of points (x_i, y_i) with no two x_i values equal, the Lagrange polynomial is the polynomial of lowest degree that assumes at each value x_i the corresponding value y_i, so that the functions match at each point. The following are the procedure's headlines:

The initial value problem is [1]:

$$_0^{ABC}D_t^z x(s) = g(s, x(s)), \quad Re(z) > 0, \quad z \in \mathbb{C}, 0 < s \leq T, \quad (9)$$

$$x(0) = x_0.$$

Because of fractional calculus's fundamental theorem with (5), we have

$$x(s) - x(0) = \frac{1}{2\pi i}(\frac{1-z}{B(z)} g(s, x(s)) + \frac{z}{B(z)+\Gamma(z)} \int_0^s g(\theta, x(\theta))(s-\theta)^{z-1} d\theta). \quad (10)$$

At s_{m+1}, we have

$$x(s_{m+1}) - x(0) = \frac{1}{2\pi i}(\frac{\Gamma(z)(1-z)}{z+\Gamma(z)(1-z)} g(s_m, x(s_m)) + \frac{z}{\Gamma(z)+z(1-\Gamma(z))}$$

$$\times \sum_{j=0}^{m} \int_{s_n}^{s_{j+1}} g(\theta, x(\theta))(s_{m+1}-\theta)^{z-1} d\theta). \quad (11)$$

Using the two-step Lagrange polynomial

$$P_k(\theta);\frac{g(s_j,x_j)}{h}(\theta-s_{j-1})-\frac{g(s_{j-1},x_{j-1})}{h}(\theta-s_j). \tag{12}$$

When we insert Eq.(12) into (11) and follow the same steps as in [9] we obtain:

$$x_{m+1}(s)=x(0)+\frac{1}{2\pi i}\left(\frac{(1-z)\Gamma(z)}{z+\Gamma(z)(1-z)}g(s_m,x(s_m))+\frac{1}{(z+1)(1-z)\Gamma(z)+z}\right.$$

$$\times\sum_{j=0}^{m}(h^z g(s_j,x_j)((m+1-j)^z(m-j+2+z)-(m-j)^z(m-h$$

$$+2+2z))-h^z g(s_{j-1},x_{j-1})((1+m-j)^{z+1}-(m-j)^z$$

$$\left.\times(1-j+m+z))\right). \tag{13}$$

We employed a simple modulation in (13) to get good stability [31]. Changing the step size h is the purpose of this modulation to $\phi(h)$ as a result $\phi(h)=h+O(h^2)$, $0<\phi(h)\le 1$. For more details see ([25],[26], [28], [29], [30]).

Below is an illustration of the non-standard two-step Lagrange interpolation method (NS2LIM):

$$x_{m+1}(s)=x(0)+\frac{1}{2\pi i}\left(\frac{\Gamma(z)(1-z)}{z+\Gamma(z)(1-z)}g(s_m,x(s_m))+\frac{1}{z+(z+1)(1-z)\Gamma(z)}\right.$$

$$\times\sum_{j=0}^{m}(\phi(h)^z g(s_j,x_j)((m+1-j)^z(m-j+2+z)-(m-j)^z(m-j$$

$$+2+2z))-\phi(h)^z g(s_{j-1},x_{j-1})((1+m-j)^{z+1}-(m-h)^z$$

$$\left.\times(1-j+m+z))\right). \tag{14}$$

6 Numerical Scheme

The system (7) is represented numerically as follows using the NS2LIM (14):

$${}_0^{ABC}D_s^{e+if}T(s)=g_1,\quad {}_0^{ABC}D_s^{e+if}T_s(s)=g_2,\quad {}_0^{ABC}D_s^{e+if}V_s(s)=g_3,$$

$${}_0^{ABC}D_s^{e+if}T_r(s)=g_4,\quad {}_0^{ABC}D_s^{e+if}V_r(s)=g_5,$$

$${}_0^{ABC}D_s^{e-if}T(s)=g_1^*,\quad {}_0^{ABC}D_s^{e-if}T_s(s)=g_2^*,\quad {}_0^{ABC}D_s^{e-if}V_s(s)=g_3^*,$$

$${}_0^{ABC}D_s^{e-if}T_r(s)=g_4^*,\quad {}_0^{ABC}D_s^{e-if}V_r(s)=g_5^*,$$

where

$$g_k=g(s,T,T_s,V_s,T_r,V_r),$$

$$g_k^j:=g(s,T^j,T_s^j,V_s^j,T_r^j,V_r^j),$$

$$g_k^m:=g(s,T^m,T_s^m,V_s^m,T_r^m,V_r^m),$$

$$g_k^* = g^*(s,T,T_s,V_s,T_r,V_r),$$

$$g_k^{*^m} := g^*(s,T^m,T_s^m,V_s^m,T_r^m,V_r^m),$$

$$g_k^{*^j} := g^*(s,T^j,T_s^j,V_s^j,T_r^j,V_r^j),$$

$$k = 1,...,5.$$

$$T_{m+1}(s) = T(0) + \frac{1}{4\pi i} * (\frac{\Gamma(e+if)(1-(e+if))}{\Gamma(e+if)(1-(e+if))+(e+if)} g_1^m +$$

$$\frac{2}{(e+if)+(1-(e+if))((e+if)+1)\Gamma(e+if)} \sum_{j=0}^{m} (g_1^j \phi(h)^{e+if} ((1+m-j)^{e+if}$$

$$\times (m+2-j+(e+if)) - (m+2-j+2(e+if))(m-j)^{e+if}) - \phi(h)^{e+if}$$

$$\times g_1^{j-1}((1+m-j)^{(e+if)+1} - (1-j+m+(e+if))(m-j)^{(e+if)}))) +$$

$$(\frac{\Gamma(e-if)(1-(e-if))}{\Gamma(e-if)(1-(e-if))+(e-if)} g_1^{*^m} + \frac{1}{\Gamma(e-if)(1-(e-if))((e-if)+1)+(e-if)}$$

$$\times \sum_{j=0}^{m} (\phi(h)^{e-if} g_1^{*^j} \phi(h)^{e-if} ((1+m-j)^{e-if} (2+m-j+(e-if)) - (m-j)^{e-if} (m-j+2$$

$$+ 2(e-if))) - \phi(h)^{e-if} g_1^{*^{j-1}} ((1+m-j)^{(e-if)+1} - (1-j+m+(e-if))(m-j)^{(e-if)}))) * (1/4\pi i).$$

$$T_{s_{m+1}}(s) = T_s(0) + \frac{1}{4\pi i} * (\frac{\Gamma(e+if)(1-(e+if))}{\Gamma(e+if)(1-(e+if))+(e+if)} g_2^m +$$

$$\frac{2}{(e+if)+(1-(e+if))((e+if)+1)\Gamma(e+if)} \sum_{j=0}^{m} (g_2^j \phi(h)^{e+if} ((1+m-j)^{e+if}$$

$$\times (m+2-j+(e+if)) - (m+2-j+2(e+if))(m-j)^{e+if}) - \phi(h)^{e+if}$$

$$\times g_2^{j-1}((1+m-j)^{(e+if)+1} - (1-m+1+(e+if))(m-j)^{(e+if)}))) +$$

$$(\frac{\Gamma(e-if)(1-(e-if))}{\Gamma(e-if)(1-(e-if))+(e-if)} g_2^{*^m} + \frac{1}{\Gamma(e-if)(1-(e-if))((e-if)+1)+(e-if)}$$

$$\times \sum_{j=0}^{m} (\phi(h)^{e-if} g_2^{*^j} \phi(h)^{e-if} ((1+m-j)^{e-if} (2+m-j+(e-if)) - (m-j)^{e-if} (m-j+2$$

$$+ 2(e-if))) - \phi(h)^{e-if} g_2^{*^{j-1}} ((1+m-j)^{(e-if)+1} - (1-j+m+(e-if))(m-j)^{(e-if)}))) * (1/4\pi i).$$

$$V_{s_{m+1}}(s) = V_s(0) + \frac{1}{4\pi i} * (\frac{\Gamma(e+if)(1-(e+if))}{\Gamma(e+if)(1-(e+if))+(e+if)} g_3^m +$$

$$\frac{2}{(e+if)+(1-(e+if))((e+if)+1)\Gamma(e+if)} \sum_{j=0}^{m} (g_3^j \phi(h)^{e+if} ((1+m-j)^{e+if}$$

$$\times (m+2-j+(e+if)) - (m+2-j+2(e+if))(m-j)^{e+if}) - \phi(h)^{e+if}$$

$$\times g_3^{j-1} ((1+m-j)^{(e+if)+1} - (1-j+m+(e+if))(m-j)^{(e+if)}))) +$$

$$(\frac{\Gamma(e-if)(1-(e-if))}{\Gamma(e-if)(1-(e-if))+(e-if)} g_3^{*m} + \frac{1}{\Gamma(e-if)(1-(e-if))((e-if)+1)+(e-if)}$$

$$\times \sum_{j=0}^{m} (\phi(h)^{e-if} g_3^{*j} \phi(h)^{e-if} ((1+m-j)^{e-if} (2+m-j+(e-if)) - (m-j)^{e-if} (m-j+2$$

$$+ 2(e-if))) - \phi(h)^{e-if} g_3^{*j-1} ((1+m-j)^{(e-if)+1} - (1-j+m+(e-if))(m-j)^{(e-if)}))) * (1/4\pi i).$$

$$T_{r_{m+1}}(s) = T_r(0) + \frac{1}{4\pi i} * (\frac{\Gamma(e+if)(1-(e+if))}{\Gamma(e+if)(1-(e+if))+(e+if)} g_4^m +$$

$$\frac{2}{(e+if)+(1-(e+if))((e+if)+1)\Gamma(e+if)} \sum_{j=0}^{m} (g_4^j \phi(h)^{e+if} ((1+m-j)^{e+if}$$

$$\times (m+2-j+(e+if)) - (m+2-j+2(e+if))(m-j)^{e+if}) - \phi(h)^{e+if}$$

$$\times g_4^{j-1} ((1+m-j)^{(e+if)+1} - (1-j+m+(e+if))(m-j)^{(e+if)}))) +$$

$$(\frac{\Gamma(e-if)(1-(e-if))}{\Gamma(e-if)(1-(e-if))+(e-if)} g_4^{*m} + \frac{1}{\Gamma(e-if)(1-(e-if))((e-if)+1)+(e-if)}$$

$$\times \sum_{j=0}^{m} (\phi(h)^{e-if} g_4^{*j} \phi(h)^{e-if} ((1+m-j)^{e-if} (2+m-j+(e-if)) - (m-j)^{e-if} (m-j+2$$

$$+ 2(e-if))) - \phi(h)^{e-if} g_4^{*j-1} ((1+m-j)^{(e-if)+1} - (1-j+m+(e-if))(m-j)^{(e-if)}))) * (1/4\pi i).$$

$$V_{r_{s+1}}(s) = V_r(0) + \frac{1}{4\pi i} * (\frac{\Gamma(e+if)(1-(e+if))}{\Gamma(e+if)(1-(e+if))+(e+if)} g_5^m +$$

$$\frac{2}{(e+if)+(1-(e+if))((e+if)+1)\Gamma(e+if)} \sum_{j=0}^{m} (g_5^j \phi(h)^{e+if} ((1+m-j)^{e+if}$$

$$\times (m+2-j+(e+if)) - (m+2-j+2(e+if))(m-j)^{e+if}) - \phi(h)^{e+if}$$

$$\times g_5^{j-1} ((1+m-j)^{(e+if)+1} - (1-j+m+(e+if))(m-j)^{(e+if)}))) +$$

$$\left(\frac{\Gamma(e-if)(1-(e-if))}{\Gamma(e-if)(1-(e-if))+(e-if)}\,g_5^{*m}+\frac{1}{\Gamma(e-if)(1-(e-if))((e-if)+1)+(e-if)}\right.$$

$$\times\sum_{j=0}^{m}(\phi(h)^{e-if}\,g_5^{*j}\,\phi(h)^{e-if}((1+m-j)^{e-if}(2+m-j+(e-if))-(m-j)^{e-if}(m-j+2$$

$$\left.+2(e-if)))-\phi(h)^{e-if}\,g_5^{*j-1}((1+m-j)^{(e-if)+1}-(1-j+m+(e-if))(m-j)^{(e-if)}))*(1/4\pi i).\right.$$

7 Numerical Results

Following are presented numerical simulations of the complex HIV model. The initial conditions are $T=1000$, $T_s=1$, $V_s=0.01$, $T_r=0.01$, $V_r=0.01$. Table 3 details how the numerical algorithms NS2LIM, S2LIM, and Ode45 behave in terms of convergence when e = 1 and f = 0. The CPU time shows in Table 4 when $e=0.9$ and $f=0.2$. Figure 1, displays how the behaviour of Infected $CD4^+T$ drug-sensitive cells and Infected $CD4^+T$ drug-resistant cells at $1+0i$, $1+0.21i$ with $k_s=2.4*10^{-5}$, $k_r=2*10^{-5}$ and rate of growth G_1 using NS2LIM. Figure 2, represented how the behaviour of Uninfected $CD4^+T$ populations cells at different values $u\pm v$ with $k_s=2.4*10^{-5}$, $k_r=2*10^{-5}$ and rate of growth G_1 using NS2LIM. Figure 3, portrays the behaviour of Infected $CD4^+T$ drug-sensitive cells and Infected $CD4^+T$ drug-resistant cells at at different values $u\pm v$ with $k_s=2.4*10^{-5}$, $k_r=2*10^{-5}$ and rate of growth G_1 using NS2LIM. Figure 4, displays the behaviour of Infectious viruses of drug-resistant and Infectious viruses of drug-sensitive at different values of $u\pm v$ with $k_s=2.4*10^{-5}$, $k_r=2*10^{-5}$, $u=3*10^{-8}$ and rate of growth G_1 using NS2LIM. Figure 5, displays the behaviour of Uninfected $CD4^+T$ populations cells at different values $u\pm v$ with $k_s=2.4*10^{-5}$, $k_r=2*10^{-5}$, $u=3*10^{-8}$ and rate of growth G_2 using NS2LIM.

Table 3: Comparisons between NS2LIM, S2LIM, Ode45 and $s_{final}=1000$ at different various of h, $e=1$, $f=0$.

h	NS2LIM	S2LIM	Ode45
0.2	Convergent	Convergent	Convergent
3	Convergent	Convergent	Convergent
6	Convergent	Divergent	Divergent
20	Convergent	Divergent	Divergent
30	Convergent	Divergent	Divergent
50	Convergent	Divergent	Divergent

Table 4: The CPU time when $e=0.8$, $f=0.25$.

t_{final}	NS2LIM CPU time	S2LIM CPU time
200	0.3758 sec	1.4714 sec
900	0.42154 sec	2.562173 sec
3000	0.56262 sec	4.623946 sec
6000	0.536201 sec	22.432765 sec

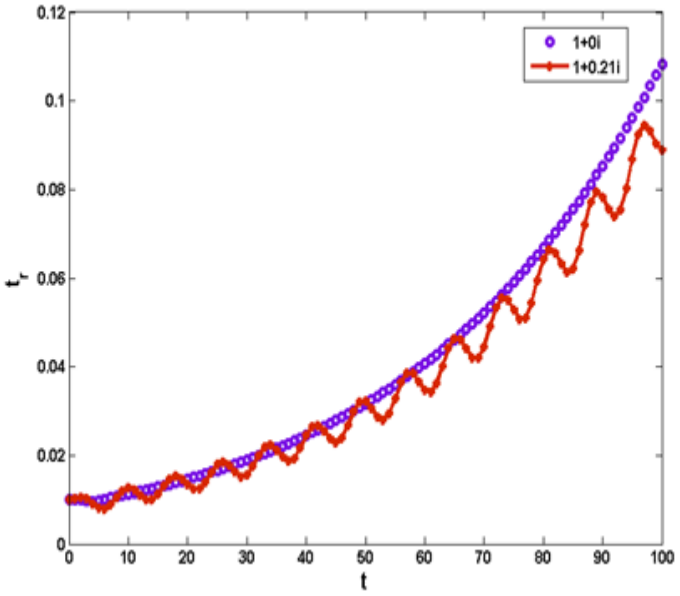

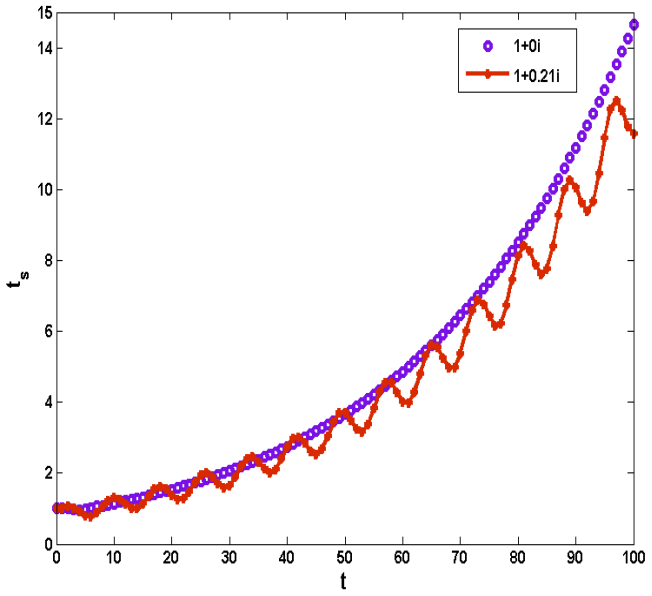

Figure 1: Numerical simulation of t_r and t_s with $k_s = 2.4*10^{-5}$, $k_r = 2*10^{-5}$ and growth rate G_1 using NS2LIM.

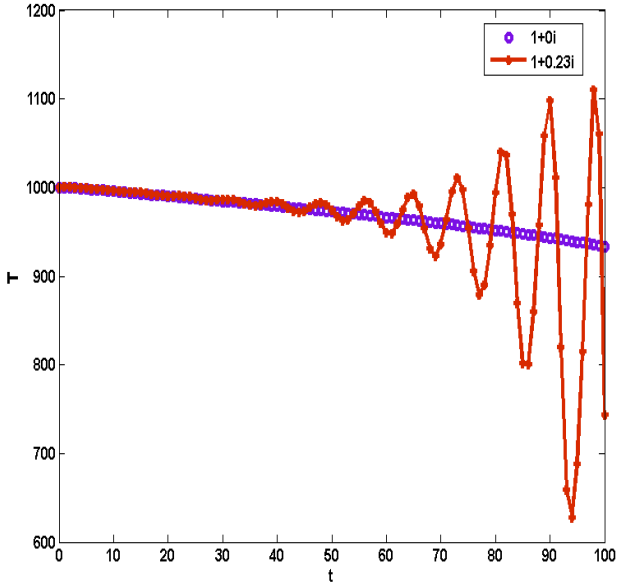

Figure 2: Numerical simulation of T with $k_s = 2.4*10^{-5}$, $k_r = 2*10^{-5}$ and growth rate G_1 using NS2LIM.

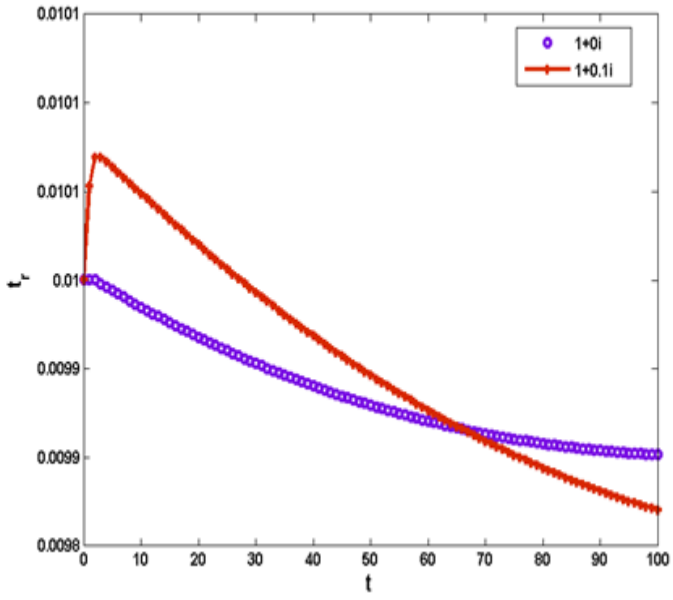

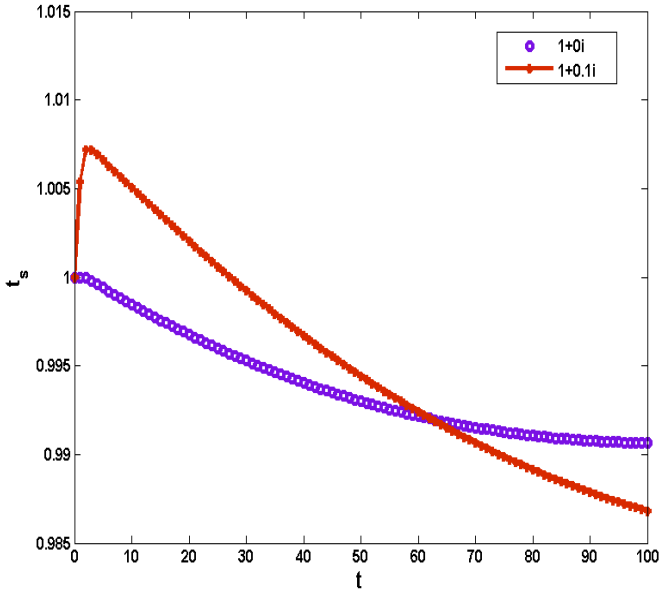

Figure 3: Numerical simulation of t_r, t_s with $k_s = 2.4*10^{-5}$, $k_r = 2*10^{-5}$ and growth rate G_1 using NS2LIM.

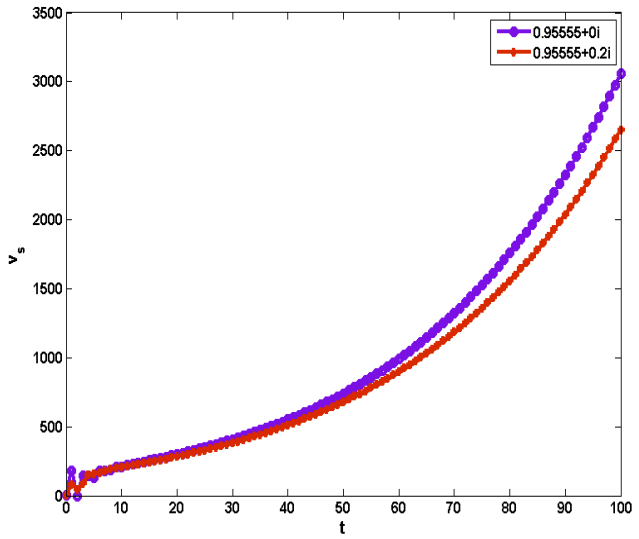

Figure 4: Numerical simulation of V_r and V_s with $k_s = 2.4*10^{-5}$, $k_r = 2*10^{-5}$, $u = 3*10^{-8}$ and growth rate G_1 using NS2LIM.

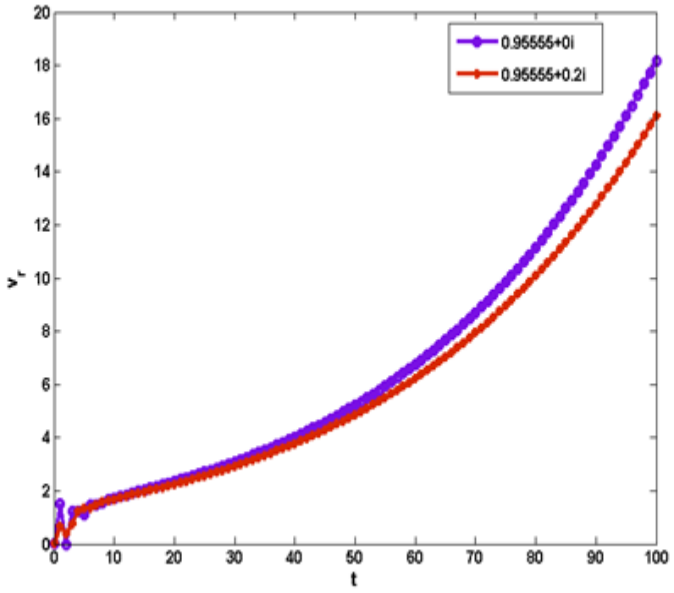

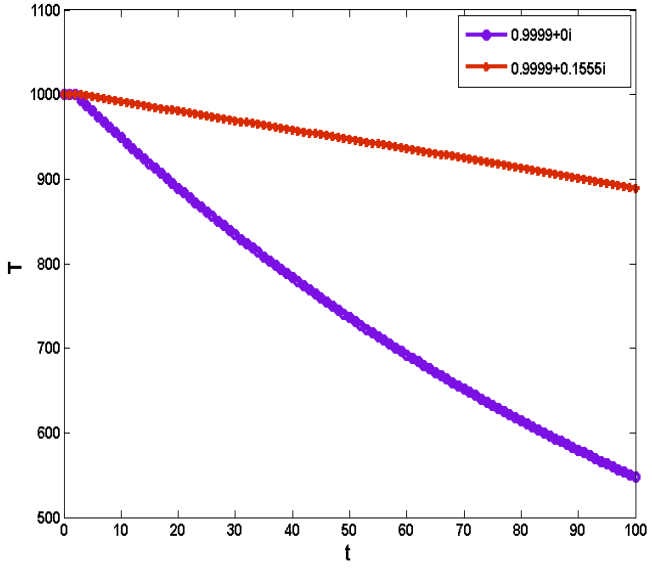

Figure 5: Numerical simulation of T with $k_s = 2.4*10^{-5}$, $k_r = 2*10^{-5}$, $u = 3*10^{-8}$ and growth rate G_2 using NS2LIM.

8 Conclusions

The mathematical model for HIV complex order is discussed in this article. It is easier to depict biological processes with memory using this dynamical model. The complex-order system also exhibits a diverse range of dynamics for the complex-order derivative value. An interpolation technique based on Lagrange polynomials is employed to obtain numerical solutions for a complex order HIV model with Mittag-Leffler kernels. The approach is precise, effective, and straightforward.

References

[1] N. Sweilam, S. AL-Mekhlafi, Z. Mohammed, W. Abd kareem, Numerical Treatments for a Multi-Time Delay Complex Order Mathematical Model of HIV/AIDS and Malaria, Alexandria Engineering Journal, 10263-10276, 61(12), (2022).

[2] N. Sweilam,S. AL-Mekhlafi, Z. Mohammed, D. Baleanu, Optimal control for variable order fractional HIV/AIDS and malaria mathematical models with multi-time delay, Alexandria Engineering Journal, 3149-3162, 59(5), (2020).

[3] C. Pinto, A. Carvalho, Fractional complex-order model for HIV infection with drug resistance during therapy, Journal of Vibration and Control, 22(9), 2222-2239, (2016).

[4] Y.Xiao, H.Miao, S.Tang, et al, Modeling antiretroviral drug responses for HIV-1 infected patients using differential equation models, Advanced Drug Delivery Reviews 65, 940-953, (2013).

[5] A. Fernandez, A complex analysis approach to Atangana-Baleanu fractional calculus, J Math Methods Appl Sci, 1-18, (2019).

[6] N. Sweilam, F. Rihan, S. AL-Mekhlafi, A fractional-order delay differential model with optimal control for cancer treatment based on synergy between anti-angiogenic and immune cell therapies, Discrete Contin. Dyn. Syst, 13(9), 2403-2424, (2020).

[7] A. Neamaty, M. Yadollahzadeh, R. Darzi, On fractional differential equation with complex order, J Prog Fract Diff Appl, 223-227, (2015).

[8] N. Sweilam, S. AL-Mekhlafi, A. ALshomrani, D. Baleanu, Comparative study for optimal control nonlinear variable-order fractional tumor model, Chaos Solitons Fractals, 136, (2020).

[9] J. Solis-Pérez, J. Omez-Aguilar, Novel numerical method for solving variable-order fractional differential equations with power, exponential and Mittag-Leffler laws, Chaos Solitons Fractals, 14, 175-185, (2018).

[10] O. Agrawal, A general formulation and solution scheme for fractional optimal control problems, Nonlinear Dynam., 38, 323-337, (2004).

[11] E. Love, Fractional derivatives of imaginary order, J. London Math. Soc, 3(2), 241-259, (1971).

[12] N. Sweilam, F. Rihan, S. AL-Mekhlafi, A fractional-order delay differential model with optimal control for cancer treatment based on synergy between anti-angiogenic and immune cell therapies, Discrete and Continuous Dynamical Systems Series, 13(9), 2403-2424, (2020).

[13] N. Sweilam, S. Al-Mekhlafi, T. Assiri, A. Atangana, Optimal control for cancer treatment mathematical model using Atangana-Baleanu-Caputo fractional derivative, 1, 1-21, (2020),

[14] A. Atangana, D. Baleanu, New fractional derivatives with non-local and non-singular kernel theory and application to heat transfer model. Therm Sci, 20(2), 763-769, (2016).

[15] M. Khader, N. Sweilam, A. Mahdy, N. Abdel Moniem, Numerical simulation for the fractional SIRC model and influenza, Applied Mathematics and Information Sciences, 8(3), 1029-1036, (2014).

[16] N. Sweilam, M. Khader, M. Adel, Numerical simulation of fractional Cable equation of spiny neuronal dendrites, Journal of Advanced Research, 5(2), 253-259, (2014).

[17] A. Atangana, km. Owolabi, New numerical approach for fractional differential equations, Math Model Nat Phenom, 13(1), 1-17, (2018).

[18] D. Valerio, J. Costa, Variable-order fractional derivatives and their numerical approximations, Symposium on Fractional Signals and Systems, 4-9, (2009).

[19] A. Arafa , M. Khalil, A. Sayed, A non-Integer variable order mathematical model of human immunodeficiency virus and malaria coinfection with time delay, Hindawi Complexity, 13, (2019).

[20] G. Brown, Progress in the development of malaria vaccines: context and constraints, Parassitologia, 41, 1-3, 429-432, (1999).

[21] A. Carvalho and M. Pinto, A delay fractional order model for the co-infection of malaria and HIV/AIDS, Int. J. Dynam Control, 5, 168-186, (2017).

[22] C. Pinto, J. Machado, Complex-order forced van der Pol oscillator, J Vib Control, 18 (14), 2201-2209, (2011).

[23] D. Kazmin, H. Nakaya, E. Lee et al., Systems analysis of protective immune responses to RTS, malaria vaccination in humans, Proceedings of the National Acadamy of Sciences of the United States of America, vol. 114(9), 2425-2430, (2017).

[24] L. Miller, P. David, T. Hadley, R. Freeman, Perspectives for malaria vaccination, Philosophical Transactions of the Royal Society B: Biological Sciences, 84(2), 99-115, (1984).

[25] R. Mickens, Nonstandard Finite Difference Models of Differential Equations. World Scientific, Singapore, (2005).

[26] R. Mickens, Calculation of denominator functions for nonstandard finite difference schemes for differential equations satisfying a positivity condition, numerical methods for partial differential equations, 23, 672-691, (2007).

[27] I. Podlubny, Fractional Differential Equations, New York: Academic Press, (1999).

[28] K. Patidar, Nonstandard finite difference methods: recent trends and further developments, Journal of Difference Equations and Applications, 22(6), 817-849, (2016).

[29] N. Sweilam, I. Soliman, S. AL-Mekhlafi, Nonstandard finite difference method for solving the multi-strain TB model, Journal of the Egyptian Mathematical Society, 25(2), 129-138, (2017).

[30] N. Sweilam, S. AL-Mekhlafi, Optimal control for a nonlinear mathematical model of tumor under immune suppression: A numerical approach, Optim Control Appl Meth, 1-16, (2018).

[31] N. Sweilam, S. AL-Mekhlafi, D. Baleanu, Optimal control for a fractional tuberculosis infection model including the impact of diabetes and resistant strains, Journal of Advanced Research, 17, 125-137, (2019).

[32] M. Toufik, A. Atangana, New numerical approximation of fractional derivative with non-local and non-singular kernel, application to chaotic models, Eur Phys J Plus, 132(10),1-16, (2017).

[33] M. Caputo, The role of memory in modeling social and economic cycles of extreme events, A Handbook of Alternative Theories of Public Economics, 245-259, (2014).

[34] C. Pinto, J. Machado, Fractional model for malaria transmission under control strategies, Comput. Math. Appl, 66, 908-916, (2013).

[35] A. Saadatmandi, M. Dehghan, A new operational matrix for solving fractional-order differential equations, Comput. Math. Appl, 59, 1326-1336, (2010).

[36] R. Scherer, S. Kalla, Y. Tang, J. Huang, The Grunwald-Letnikov method for fractional differential equations, Comput. Math. Appl, 62, 902-917, (2011).

[37] N. Sweilam, S. AL-Mekhlafi, Nonstandard finite difference method for solving complex-order fractional Burgers' equations, Journal of Advanced Research, 25, 19-29, (2020).

[38] R. Abazari, M. Ganji, Extended two-dimensional DTM and its application on nonlinear PDEs with proportional delay, Int J Comput Math, 88(8), 1749-62, (2011).

[39] N. Sweilam, W. Abd kareem, S. AL-Mekhlafi, Z. Mohammed, Numerical treatments for a complex order fractional HIV infection model with drug resistance during therapy, Progress in Fractional Differentiation and Applications, 1(1), 1-13, (2020).